Daylight Dynamics 2026

Solar Tracking Platform

Winter Final Design Report

MECH 195 Senior Design Project

Quacy Moore, German Markaryan, Dean Schultz,
Izzy Bravo, Lucas Matter, and Robert Wang

Department of Mechanical Engineering
Santa Clara University
Santa Clara, California

Winter 2026 | Graduation Spring 2026

Table of Contents

Chapter 1: Motivation, Background Research, and Customer Needs

1.1 Introduction

The recent surge in demand for alternative energy sources has been driven by rising residential electricity costs and growing concern over long-term energy sustainability. Solar photovoltaic (PV) systems have emerged as a primary solution for residential energy generation, offering a viable path toward energy independence. However, the most common deployment of these systems relies on stationary roof-mounted panels, which carry a fundamental limitation: they cannot adjust their orientation to follow the sun's path across the sky.

This fixed geometry means that energy capture is only optimal during a narrow window of the day when incident sunlight is roughly perpendicular to the panel surface. Beyond that, cosine losses reduce output substantially. Compounding this, environmental factors such as dust, pollen, and debris accumulate on panel surfaces, reducing photovoltaic efficiency by up to 30% through shading and increased cell operating temperature [1]. These inefficiencies represent a significant untapped opportunity for a system that combines active solar tracking with automated maintenance.

Despite growing adoption, solar energy still faces barriers for residential homeowners: high capital costs, uncertain return on investment (ROI), and ongoing maintenance demands. The market lacks a commercially accessible, roof-mountable solution that integrates tracking with self-cleaning at a residential scale. This project targets that gap directly.

1.2 Current Technologies

1.2.1 Fixed vs. Tracking Systems

Fixed solar panel mounts dominate the residential market due to their mechanical simplicity, low profile, and established installation practices. While reliable, they sacrifice significant energy yield by maintaining a static orientation throughout the day. Commercial and industrial applications have adopted single and dual-axis solar trackers to address this, with dual-axis configurations demonstrating 22-23% higher energy output compared to fixed installations [2]. The trade-off is substantial: existing tracker systems are bulky, heavy, and designed for ground mounting, making them impractical for the average residential rooftop.

1.2.2 Maintenance

Solar panel maintenance remains largely manual and inconsistent in residential settings. The efficiency penalty from soiling is well-documented: autonomous cleaning systems combining cooling and cleaning modules have demonstrated 14-20% efficiency recovery, while compressed air-based systems have shown 10% or greater production increases [3]. Despite this evidence, no commercially available residential solution

integrates both automated tracking and self-cleaning in a single roof-mountable package.

1.3 Future Technologies

The next generation of residential solar technology is converging around two themes: smart monitoring and modular design. Real-time energy monitoring, fault notification, and grid-connectivity are increasingly expected features rather than premium add-ons. Modularity is equally important, enabling homeowners to start with a minimal system and scale incrementally without replacing core infrastructure. These trends directly inform the Daylight Dynamics design philosophy.

1.4 Project Overview

1.4.1 Project Goal

The Daylight Dynamics team aims to develop a roof-mounted, single-axis solar tracking platform with an integrated self-cleaning subsystem that delivers a cost-effective ROI within 5-8 years. The system targets a 20-50% efficiency improvement over comparable fixed-panel installations and is designed specifically for residential deployment constraints.

1.4.2 Specific Objectives

Three core design objectives drive the project:

- High Efficiency, Short ROI: Active single-axis tracking maximizes daily energy capture, offsetting system cost through accelerated payback.
- Low Maintenance: An automated hose-fed sprinkler system eliminates the need for manual panel cleaning, directly addressing the primary residential adoption barrier.
- Roof-Mount Compatibility: The structural frame is designed to be lightweight, low-profile, and compliant with residential rooftop loading and aesthetic constraints.

1.5 Literature Review and Resource Collection

A targeted literature review was conducted to assess technical feasibility and inform design decisions across the three primary subsystems. Key findings are summarized below:

- Geetha et al. (2024): Quantified efficiency losses from dust accumulation at up to 30%, establishing the case for automated cleaning. Self-cleaning systems with spray-based mechanisms recovered 14-20% of lost efficiency [1].
- Harazin and Wrobel (2022): Analyzed prototype roof-mounted solar trackers with linear actuators and documented a 22-23% energy increase over fixed panels, directly validating the rotation mechanism approach [2].
- Li et al. (2021): Compared compressed air and water-based cleaning approaches, with compressed air achieving a 10%+ production gain. The

water-based approach was ultimately selected for this project based on feasibility and integration constraints [3].

- Ismail et al. (2020): Validated the use of Arduino microcontrollers for dual-axis solar tracking, confirming that sensor-driven panel alignment reliably improves power delivery [4].
- Almusaied et al. (2018): Highlighted that panel cleanliness and optimal orientation angle both independently contribute to peak production, reinforcing the dual-function design strategy [5].
- Melis et al. (2014): Investigated water cooling systems for thermal loss prevention, reporting a 12% gain. This finding is relevant to future iterations that may incorporate combined cleaning and cooling cycles [6].

1.6 Stakeholder Analysis

1.6.1 Stakeholder Identification

Three primary stakeholder groups were identified:

- Primary Customer (Residential Homeowner): Cost-sensitive, prioritizes short payback periods (5-8 years), system longevity, and minimal maintenance requirements.
- Secondary Customer (Aesthetics-Sensitive Homeowner): Values low visual profile and roofline integration over marginal performance gains.
- Broader Stakeholders (HOAs and Utility Organizations): Influence aesthetic and structural compliance requirements, and regulate grid interconnection eligibility.

1.6.2 Customer Needs Assessment

Structured interviews with four potential residential customers identified consistent adoption barriers. Financial concerns dominated: all respondents wanted a clearly defined payback window between 5-8 years. Maintenance was a close second, with respondents willing to pay a 5-20% premium for fully automated cleaning. Aesthetics emerged as a real constraint, not a preference, with customers specifically resistant to systems that extend noticeably above the roofline. Modularity was universally desired, with customers wanting to start small and scale without replacing core components.

1.6.3 Benchmarking

A competitive analysis was conducted against two categories of existing solutions: the ECO-WORTHY Dual-Axis Kit (commercial tracker) and standard Q-CELLS residential fixed panels.

- Commercial Dual-Axis Trackers: Achieve 30-50% energy gains but require ground mounting, carry large visual footprints, and are not compatible with typical residential rooflines.
- Fixed Residential Panels: Low-profile and widely deployed but deliver zero tracking gain and require manual maintenance.

- Gap: No commercially available solution combines active tracking, automated cleaning, and roof-mount compatibility at a residential price point.

1.6.4 Summarizing Customer Needs

Based on customer interviews and benchmarking analysis, five core design requirements were defined:

1. Financial Viability: Deliver ROI within 5-8 years through optimized cost-performance tradeoffs.
2. Operational Stability: Achieve zero-hassle operation with integrated automated self-cleaning.
3. Site Integration: Maintain roof-mount compatibility with a low-profile, unobtrusive structural footprint.
4. Scalability: Support modular expansion from 1 to 4+ panels without requiring system-level redesign.
5. User Transparency: Provide real-time energy monitoring and fault notification via internet connectivity.

1.6.5 Prioritizing Needs

Based on customer pain points and engineering constraints, project prioritization focuses on Financial Viability, Operational Stability, and Site Integration.

- Priority 1 (ROI): The additional energy production from single-axis tracking is primarily technical and helps offset costs and prolong system payback times.
- Priority 2 (Maintenance): The importance of the self-cleaning system cannot be overstated with regard to reducing or eliminating the main adoption barrier, which is maintenance.
- Priority 3 (Aesthetics/Mounting): Unlike ground-mount competitive systems, it is necessary that it be light and strong enough to be effectively roof-mounted as required in residential markets.

Chapter 2: System Definition & requirements, general system description, and subsystem decomposition.

2.1 High-Level System Overview

The goal of this project is to design, test, and prototype a modular, single-axis, roof-mounted solar tracking platform intended for residential homeowners as a consumer product. The system goal is to increase the long term efficiency of the solar panel system and hence yield a shorter return on investment, making it a competitive solar panel solution while remaining visually appealing, reliable, and with minimal maintenance.

The project target is to implement three primary functionality capabilities. Modular design is the new major change in the product design from the original design of the previous team. Modularity should allow the homeowner to scale their solar panel system from one to at least 8 solar panels. This feature will provide homeowners with an option to have a low entry barrier to test for themselves how well solar panels will work for them. It will also allow customers to buy more solar panels, scaling their power production, increasing the revenue from additional purchases, while giving homeowners an option to make a cheaper solar system per watt generated using large-scale advantages. This means that solar panel models should work well together and do not have parts, attachments, or logistics that would prevent a homeowner from scaling to any number of solar panels without buying new logic, electrical, or power systems.

The second main function of the product is a self-cleaning capability. The technology and prototype were developed by the previous team, and there are still areas for improvement to increase their efficiency. The main reason this system is important is that we want to increase the long-term efficiency of the solar panels by eliminating losses from soiling factors.

The third main function of our solar platform is automated solar tracking capabilities. Our solar tracking will be based solely on two photoresistors, so the platform can only move along one axis. This allows us to simplify the system design, making it not only cheaper but also lighter and more reliable. Two photoresistors will output a signal to the microcontroller, which will determine which photoresistor has the higher light intensity and hence turn the solar panels toward the light source. This will increase power generation efficiency, since solar beams will hit the solar panels at a smaller angle. This system will be controlled using a microcontroller that will have an algorithm designed for energy savings to ensure that turning the solar panels towards the sun produces more energy than is spent on turning the system towards the sun.

The system is not going to replace or compete with photovoltaic panels, but rather serve as an electromechanical platform that enhances their performance, helping to get the most out of them. Our team's goal is not only to prove the idea by making a concept but also to make it a consumer product that homeowners will be interested in buying. Hence, in addition to making the solar tracking platform work, we need to work

in detail on the system's roof load and legal restrictions, visual footprint, reliability, maintenance and installation instructions.

2.2 System Requirements

Table 2.1 contains requirements sorted by their types. The first type of requirement is a functional list, which specifies targets that must be met to make our product successful. These requirements were derived from the interview of California homeowners and internal engineering assessments. The second category is Performance and economic requirements, which will contain quantifiable and engineering goals. Structural and integration requirements are intended to ensure that our solar tracking platform can be legally installed on residential roofs in a straightforward manner, minimizing installation costs while ensuring safety throughout its life cycle. Finally, modularity and expandability requirements are intended to ensure our design remains scalable, enabling low-risk investment in solar panel systems for homeowners.

Table 2.1: System Requirements

Req #	Requirement	Verification
Functional Requirements		
FR-01	The system must increase the energy yield of the fixed solar panel.	Analysis & Testing
FR-02	The system must track the sun's location without human intervention.	Demonstration
FR-03	The system must clean itself without human intervention.	Demonstration
FR-04	The system must operate in daily cycles without human intervention.	Demonstration
FR-05	The system must support from 1 to 4 solar panels.	Inspection
FR-06	The system must provide operational data to the customer via internet connectivity.	Demonstration
Performance & Economic Requirements		
PR-01	The system must produce 20% more net energy than competitive solar systems.	Testing
PR-02	The system must have a return on investment shorter than 8 years.	Analysis
PR-03	The cleaning subsystem must increase the efficiency of the solar panels by at least 10%.	Testing
Structural & Integration Requirements		
SR-01	The platform must be mounted to the roof rafters.	Inspection
SR-02	The system must remain low-profile and neutral.	Demonstration
SR-03	The system must withstand 140 mph winds.	Analysis

Req #	Requirement	Verification
SR-04	The system must meet ingress protection rating IP65.	Analysis
SR-05	The system must not exceed the residential roof load limit.	Analysis
SR-06	The system must use corrosion-resistant materials for all exposed parts.	Inspection
Modularity & Expandability Requirements		
MR-01	Adding solar panel modules must not require changes to the control unit hardware or software.	Demonstration
MR-02	Adding solar panel modules must not require removal of existing parts.	Inspection
MR-03	Adding solar panel modules must not require the purchase of additional parts.	Inspection

2.3 General System Description

The Automated Tracking Light Acquisition System (ATLAS) is a roof-mounted single-axis electromechanical solar-tracking platform that supports standard-market solar panels designed for roof use. The platform will have integrated tracking and cleaning subsystems. Our product will include a single control box that controls the subsystems of each solar tracking module, which contains one solar panel per module. These modules include all-in-one package solutions for both electromechanical movement, allowing solar tracking and cleaning systems, which are connected to a unified control box, so they can work in tandem with numerous other packages.

2.3.1 Mechanical Structure

The mechanical structure consists of three nested layers. The base frame anchors to roof rafters and provides the rigid foundation for the entire assembly. A lifting mechanism built around aluminum hinges and dual linear actuators enables controlled single-axis rotation. A solar panel frame mounted on top of the lifting mechanism accepts standard residential panel sizes. The system is designed to rest flat (neutral position) when not actively tracking, minimizing wind load and visual profile during low-light conditions.

2.3.2 Self-Cleaning System

The self-cleaning system operates on a preset time interval and requires no homeowner input. When triggered, the system positions the panel at a cleaning angle and activates a hose-fed water sprayer to flush accumulated debris. Water-based cleaning was selected over mechanical brush or compressed-air alternatives to avoid surface damage and reduce maintenance of the cleaning hardware itself.

2.3.3 Tracking mechanism

Solar tracking uses a pair of photoresistors mounted with a divider between them to detect differential light intensity across the panel's axis. The microcontroller reads the

photoresistor outputs and determines whether panel rotation is warranted. If the differential exceeds a set tolerance threshold, the actuators adjust panel angle toward the brighter sensor. If neither photoresistor detects sufficient light, the system enters standby and returns to neutral. This closed-loop strategy operates without geographic data or internet connectivity, simplifying installation and enabling off-grid operation.

2.3.4 Electrical & Control System

The control unit coordinates all subsystems from a single enclosure. A microcontroller processes photoresistor inputs, executes the tracking algorithm, and issues commands to the actuators and cleaning relay. Power control electronics manage load switching for the water pump and linear actuators. A communication module provides internet connectivity, enabling the homeowner to monitor panel orientation, energy output trends, and system fault codes remotely.

2.4 Subsystem Decomposition/Breakdown

ATLAS is decomposed into five independently maintainable subsystems:

1. Panel Holder Subsystem
2. Structural Frame and Rotation Mechanism Subsystem
3. Self-Cleaning Subsystem
4. Electronics and Control Subsystem

Each subsystem is designed for independent replacement or upgrade, enabling efficient fault recovery and iterative development throughout the prototyping phase.

Chapter 3: Automatic Rotation Mechanism

3.1 Detailed Subsystem Description

One of the main objectives for our solar tracker project is to have the ability to automatically adjust its panels to optimize sunlight levels. Existing solar tracker systems with the ability to self-adjust have been shown to increase output levels by up to 22-23% [2], validating the development of such a system where fixed panels are typically implemented.

Existing solar tracking technology is minimal, mostly being limited to large ground-mounted systems. There are no market-ready options for mounting on residential roofs, mostly due to the bulky nature of tracking systems, increased weight, complexity, and visual footprint on rooftops.

The rotation mechanism subsystem utilizes the constant input from the photoresistors and control system to adjust the angle of every solar panel individually along its long axis. The design features a pair of linear actuators and sturdy hinges to make each rotation as power-efficient as possible, while still having a mechanically simple design to maximize cost efficiency and increase reliability in order to hit all engineering requirements, such as being light enough to mount on house roof rafters, having a low aesthetic profile, and being sturdy enough to resist inclement weather conditions.

3.2 Trade-off Analysis

The two most promising designs were sketched out for visualization. The first, demonstrated in **Figure 3.1** (left), was to use a single stepper gearmotor and drivetrain system connected to up to four individual panels. Each panel would have its own set of photovoltaic sensors that would feed into the central control system. The motor, through a series of propshafts and power-splitting differentials, would power a series of mechanical lifting mechanisms such as a triangle jack to lift one end of each panel. In theory, this design would be highly modular, only requiring one motor and set of electronics for up to four panels. However, the design was deemed overly complex, which could result in power losses from excessive mechanical components, had a higher chance of failure/unreliability in the field, and could be less robust in high load and inclement weather conditions (e.g. rainstorm, high winds).

The other design in **Figure 3.1** (right) utilized linear actuators, which are the common power system of choice in existing technologies. Two actuators are mounted to the base frame, and they each control rotation in opposite directions along the long axis of the panel. The biggest drawback to this design is that it is not as modular, as each panel requires its own pair of actuators, and requiring two actuators for only one axis of rotation is not the most optimized design possible. However, actuators are robust and are rated to survive harsh weather conditions (while also being shielded under the panels), require a far simpler design to implement, and are readily available and very affordable.

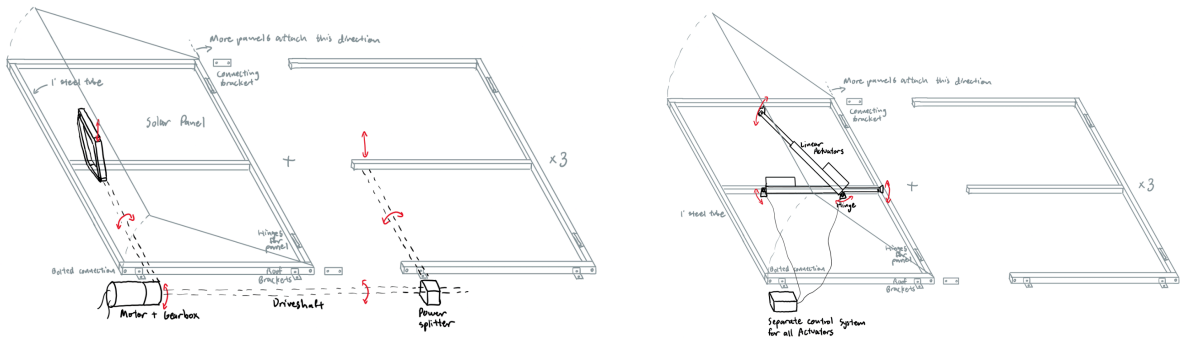

Figure 3.1: Conceptual design sketches comparing stepper motor drivetrain (left) and paired electric linear actuator (right) configurations.

In order to justify the use of one design over all others, a Pugh chart comparison table was created that compared different power systems for the rotating mechanism. The judging criteria included implementation ease, load capacity, price to implement, weight and visual profile, and maintainability and serviceability. Implementation and load capacity were weighted as the most important, as they encompassed a robust and simple design. Price and size also needed to be considered, as they were directly reflected in our customer needs.

Table 3.1: Rotation Mechanism Power System Pugh Chart

System	Impl. Ease (25%)	Load Cap. (25%)	Price (20%)	Size (20%)	Maint. (10%)	Avg (Unweighted)	Avg (Weighted)
Electric Linear Actuator	**5**	**4**	**5**	**4**	**5**	**4.6**	**4.6**
Pneumatic Piston + Air Tank	2	3	3	2	2	2.4	2.45
Servomotor + Pantograph	4	4	5	5	3	4.2	4.2
Stepper Motor + Lin. Act.	4	3	5	3	3	3.6	3.6
Motor + Rack and Pinion	4	4	3	3	3	3.4	3.3

From the options of pneumatic pistons, servo motors + pantograph, stepper motor + pantograph, and motor + rack and pinion, linear actuators were chosen with the highest score and knowledge that similar designs exist in some capacity.

3.3 Initial Design and CAD Development

An initial design was drafted in Solidworks CAD to visualize our chosen design, as shown in **Figure 3.2**. The design featured the two linear actuators mounted to the base hinge via simple machined aluminum hinges. Two scissors hinges were mounted on the side (only one side rendered) for increased stability and to prevent the linear actuators and hinges from taking all shear loads along the long axis. The design allowed for up to 50° of rotation per side.

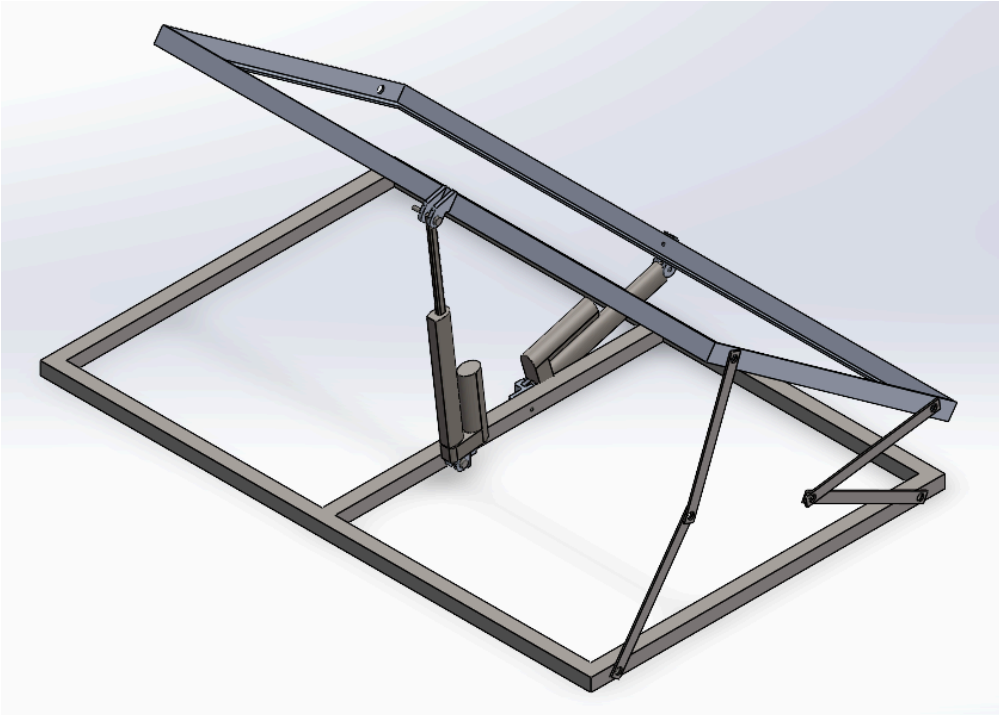

Figure 3.2: Initial SolidWorks CAD model of the rotation mechanism. *Linear actuators (center) drive panel angle via aluminum hinge brackets. Scissor hinges (sides) provide shear load distribution.*

3.4 Improved Design and Physical Manufacturing

Once the rough first design was chosen as the intended design path for the rotation subsystem, a further refined CAD was developed for a first test prototype, with realistic dimensions and manufacturability for all components considered, shown in **Figure 3.3**.

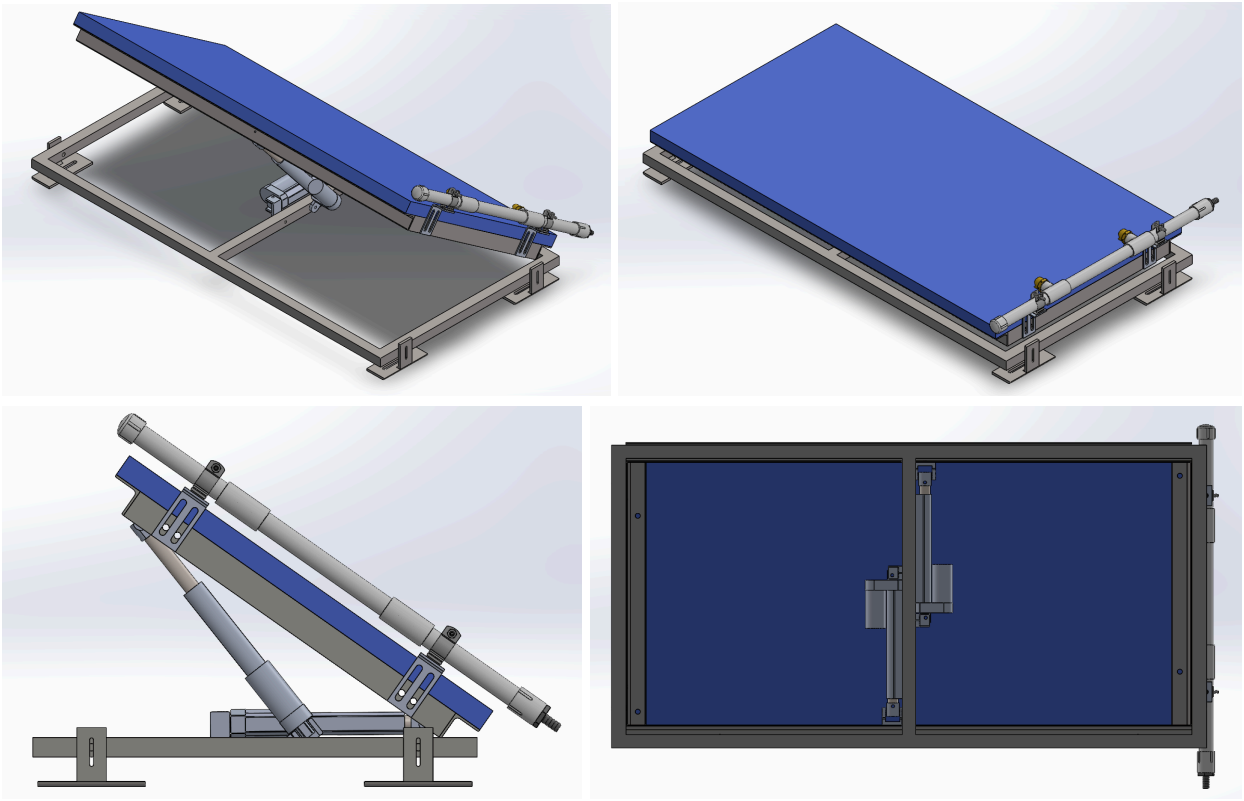

Figure 3.3: The finalized CAD of the system, in rotated up (top left) and folded down (top right) configurations, rotated up side view (bottom left), and bottom view (bottom right).

Improvements to the rotation mechanism included repositioning and re-angling the linear actuators for a more flush design. The base frame and machined hinge components were all resized or redesigned, making sure no parts would bind or interface incorrectly, although further optimization with hand calculations and FEA is required before manufacturing of the final model.

The design was built off the principle that the linear actuator's linear force would translate to rotation when applied at an angle. The solar panel sits directly on the base frame, with the linear actuators at a slight angle pointed up. When the actuator begins extending, the only free degree of movement for the solar panel is a rotation upward, as seen in the bottom left of **Figure 3.3**. Fully actuated, the panel can rotate to over 45°, although that much angle is likely unnecessary in application. The hinges that interface the actuators to the base and solar panel frames are to be machined from 6061 T6 aluminum, which provides ample strength-to-weight while remaining affordable and easy to manufacture. The frame materials are all made from mild carbon steel for affordability, as they are of very simple geometry and do not require any sophisticated machining or high strength-to-weight considerations, although other materials (such as aluminum bar) are still being considered for the final design, as the initial prototype was slightly heavy.

When the CAD design was completed, confirming all parts interacted smoothly, were manufacturable, and movement was successful, assembly of the initial rough prototype began to meet the minimum viable product requirements.

The steel tube for the base frame was cut first to dimension. Next, thick custom

3D printed brackets were made for each corner of the base frame, which would also serve as jigs for drilling the holes. The hinges for the linear actuators to connect to the frames were also 3D printed. The final versions for both the brackets and hinges will be machined, but we decided to 3D print prototypes first to ensure everything fit together, as indeed several different iterations were printed to ensure correct tolerances and sizes. The holes were then drilled and the frame assembled with bolted connections, and the linear actuators were both also bolted to the frame. Lastly, the solar panel could be mounted to each linear actuator to begin our first movement tests.

3.4 Movement Validation

One of our key goals for the minimum viable product was to be able to successfully control the rotation of the solar panel mounted on the frame. By controlling inputs of the linear actuators, the system was able to rotate under its own power, thus validating the frame's structure and movement capabilities. The entire system could modulate from flat, lowered position to maximum angle successfully, as shown in **Figures 3.4** and **3.5**.

Figure 3.4: solar panel successfully tilted

Figure 5: solar panel in its resting position, everything assembled

3.5 Future Improvements

Although technically operational, our first operational test indicated many necessary areas of improvement. The most crucial is redesigning the hinge between the solar panel frame and the linear actuator. Because the two actuators are mounted side-by-side neither pushes against the solar panel at its exact center. This causes a small bending moment, rotating the solar panel around the z-axis (up and down, perpendicular with the face of the solar panel) unintentionally. The frame hinge will need to be modified so both actuators can push directly on the center, and the scissor hinges will need to be added for extra support against unintended moments. Additionally, hand calculations and FEA, which are currently underway, will need to be completed in order to optimize the parts before final manufacturing.

Chapter 4: Automatic Self-Cleaning Subsystem

4.1 Detailed Subsystem Description

The self-cleaning system will be designed to operate automatically, regularly removing debris from the panels and thereby improving power-generation efficiency. The efficiency of solar panels can decrease by nearly 20% when dirt and other debris accumulate, blocking the sunlight from reaching the photovoltaic cells within the panels [7]. Common cleaning systems include sprinklers or brushes that sweep along the panels.

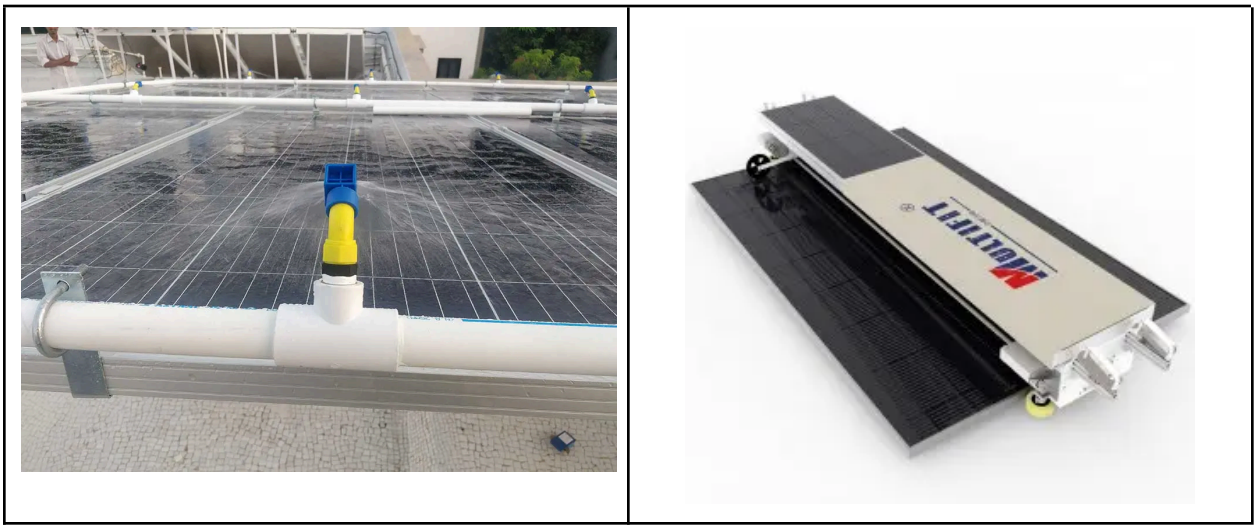

Figure 4.1: Sprinkler-Style Solar Panels Cleaning System (Left) [8] and Brush Cleaning System (Right) [9]

Ideally, the subsystem and any required components reduce the hands-on maintenance required of the consumer. However, the system is limited by the budget for the design, as well as power and possibly water consumption. The system should not damage the panels, so abrasive cleaners, such as a brush, should be avoided. The system must also be controllable through a Raspberry PI and receive power generated from the panels and battery system to keep the entire system self-contained. It must also be effective enough to remove 90% of typical dirt and debris each cleaning cycle.

4.2 Trade-off Analysis

The design of the self-cleaning subsystem is such that the system is self-contained, to aid in the maintenance of the solar panels, whilst requiring very little maintenance of its own, with the ultimate end goal of reducing the burden of care placed on the customer. As a result, the final decision-making drivers were reliability/maintenance, cleaning effectiveness, implementation cost, water consumption, and operating power; their respective weights are shown in Table 4.1. Any system that breaks, clogs, or needs specific technical maintenance is a failure. The system should remove at least 90% of debris/soil buildup when running. It should cost at most $500 and use as little power and water to operate as possible to keep the system budget and

environmentally friendly. Reliability/maintenance was weighted highest because the end goal of the subsystem is to reduce the frequency and thoroughness of maintaining the solar panel system. Cleaning effectiveness was weighted second-highest because the ability to clean will have the highest impact on power generation efficiency. Implementation cost was weighted at 20% because of the limited budget the team was allocated, along with reducing the return on investment by using cost-effective designs. Water consumption and operating power were weighted at 15% and 10%, respectively.

Table 4.1: Self-Cleaning Subsystem Decision Criteria and Weights

Decision Driver	Weight
Reliability / Maintenance	30%
Cleaning Effectiveness	25%
Implementation Cost	20%
Water Consumption	15%
Operating Power	10%

The design alternatives analyzed were a pressurized or hose-fed sprinkler system, a motorized wet wiper, a pressurized air blower, and an electrostatic cleaning system. The pressurized sprinkler system would consist of a 12V Water Diaphragm Pump that forces water from a reservoir through PVC pipes and spray nozzles. The tracker would then tilt to wash dirt and water away. The hose-fed sprinkler system is an iteration that replaces the pump and reservoir and connects directly to a garden hose. A 12V Solenoid Valve (controlled by the Raspberry PI) would open to allow pressurized water from the house to flow through the same PVC pipes and nozzles. The motorized wet wiper would consist of a 12V linear actuator or motor that moves a wiper blade across the panel, removing any particles or debris. Nozzles just ahead of the wiper would push water onto the panels, mimicking a car’s windshield wiper. The pressurized air blower replaces the water pump with a 12V high-pressure air blower to blast dust off the panel. This would be a waterless system. Finally, the electrostatic dust removal (EDS) system would require a special transparent film to be applied to the panel. A controller would send a high-voltage, low-current signal to the film, creating an electrostatic field that repels dust particles. This would be a waterless system without any moving parts. Each choice was given a score of 1-5 for each design-driver, and the weighted scores were analyzed to come to a final decision. These scores are provided in Table 4.2.

Table 4.2: Self-Cleaning System Design Alternative Pugh Chart

System	Reliability (30%)	Cleaning (25%)	Cost (20%)	Water (15%)	Power (10%)	Avg (Unwt.)	Avg (Wtd.)
Pressurized Sprinkler	2	4	3	3	3	3.0	2.95
Hose-Fed Sprinkler	**5**	**4**	**3**	**3**	**4**	**3.8**	**3.95**
Motorized Wet Wiper	3	5	2	2	4	3.2	3.25
Pressurized Air Blower	4	3	4	5	1	3.4	3.6
Electrostatic Film (EDS)	**5**	**4**	**1**	**5**	**5**	**4.0**	**3.95**

After scoring our design choices, there was a tie for first place between the Hose-fed Sprinkler and the Electrostatic Cleaning, with a score of 3.95. The Hose-fed design got its score by being a great all-rounder: cheap, reliable, and effective. The EDS system got its score by being perfect on paper. It does not use any water, has no moving parts, and does not draw a lot of power. While this seems like the obvious choice, the transparent conductive film required is hard to find, making it unsuitable for the scope of this project.

4.3 Initial CAD Design

The self-cleaning system design was based on the previous team's PVC piping with periodically spaced nozzles and brackets for mounting, which aligned with the hose-fed sprinkler alternative selected in section 4.2. One key difference between the two designs is the side of the panel on which the system will be mounted. The previous model mounted theirs on the longest side of the panels, whereas the current design will use the shortest side to accommodate the tracking system's rotation angle. This new version has two nozzles per panel, where the previous CAD design utilized four per panel. Minor changes include the specific mounting brackets chosen. The new design includes slots that allow for some maneuverability in the vertical direction. They also selected smaller nozzles, which led to a mist-like spray as opposed to the nozzles, which are slightly larger and allow for more volumetric flow to help "push" the debris off. These changes can be seen in **Figure 4.2**.

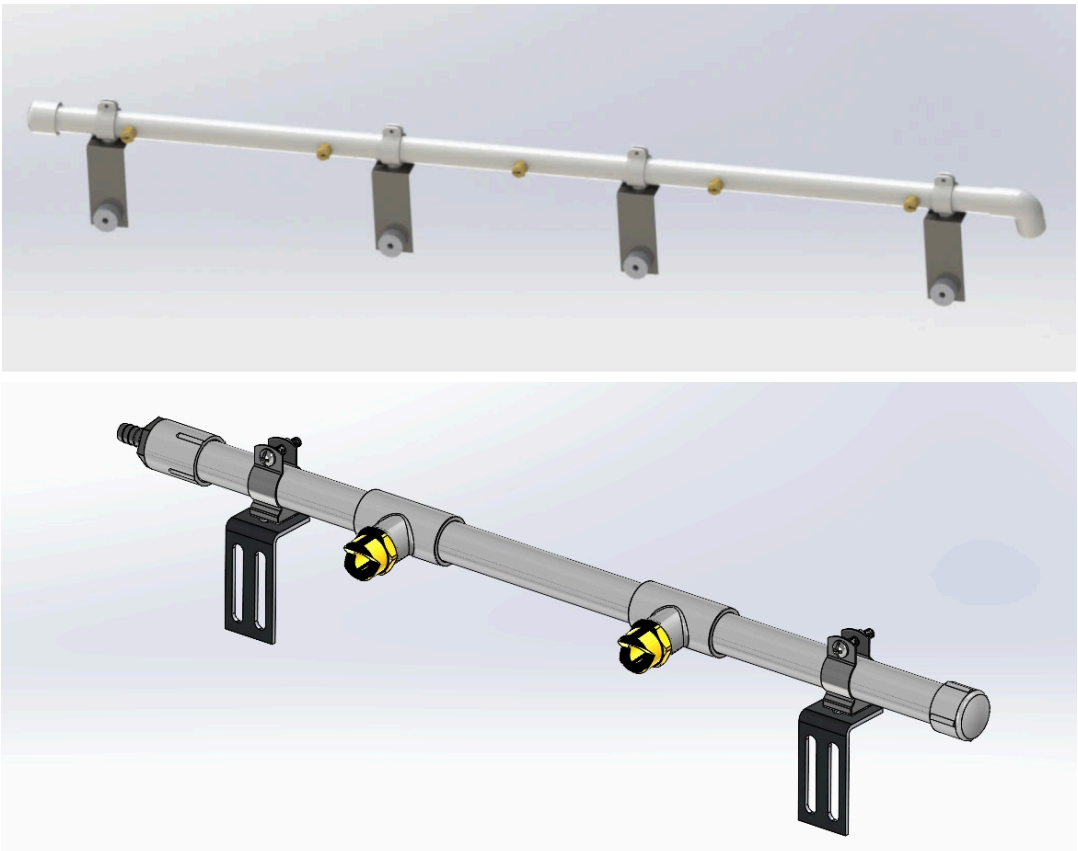

Figure 4.2: The Previous Team's Design (Top) and the New Design (Bottom) of the Self-Cleaning Subsystem

The material selection for the automatic self-cleaning subsystem was made according to the previous team's design and consists of Schedule 40 PVC pipes equipped with two brass flat-spray nozzles and reducing tee-fittings, all secured to the panel holder via metal brackets. The total cost of these materials is less than $400, further confirming the selection of the system with regard to the trade-off analysis.

4.4 Design Verification & Testing

4.4.1 Motivation and Context

The self-cleaning subsystem will be responsible for removing dirt and other debris from the panel, allowing for a higher energy production yield, boosting the system's efficiency. The efficiency of the solar panels depends heavily on their cleanliness so that UV rays can reach the photovoltaic cells. The current design uses a pump to draw water from the plumbing supply, filter it, and then spray it across the panels. However, to optimize the efficiency and eco-friendliness of the system, we aim to determine how much water is needed per cycle to clean the panels and what pressure is most efficient in removing debris from the panels. The water pressure will likely be a key factor in determining the amount of water used and the effectiveness of the cleaning system. Per manufacturer instructions, the panels should be cleaned using a damp cloth, with a warning to avoid harsh chemicals [10]. Given these instructions

and other general cleaning guidelines, pressure washing should be avoided. Light-duty pressure washing usually occurs at above 100 psi and between 1 and 2 gallons per minute, with both values increasing for more rigorous applications [11]. To avoid damaging any coatings on the panels, a lower pressure will be utilized.

This investigation will allow us to determine the cleaning effectiveness and the estimated time the system will need to run to clean debris from the panels, given the selected pump in conjunction with the nozzles. If the tests are not satisfactory, we may need to find a different pump that can achieve a higher flow rate or perhaps a different nozzle.

4.4.2 Methodology:

The current modeled system consists of schedule 40 PVC pipes, 2 brass flat-spray nozzles rated at 4.2 GPM at 20 psi, appropriate tee-fittings and endcap, and brackets that will eventually connect to the panel holder. The pump is not modeled in SolidWorks, but operates at approximately 65 psi and 1.5 gal/min. The selected nozzles have a flow rate of 6 gal/min at 40 psi and 9.4 gal/min at 100 psi. Interpolation was used to find what flow rate the nozzles would require at 65 psi, as shown in equation 1.

$$\frac{a1-a2}{b1-b2} = \frac{ax-a2}{bx-b2} \text{ or } \frac{9.4\ gal/min - 6\ gal/min}{100\ psi - 40\ psi} = \frac{x\ gal/min - 6\ gal/min}{65\ psi - 40\ psi} \text{ (Eqn. 1)}$$

The expected flow rate for the nozzles would be 7.3 gal/min at 65 psi. Using equation 1, but solving for the pressure at a flow rate of 1.5 gal/min, the expected pressure of the nozzles is -40 psi. Given this non-physical solution, the approximate value would be near 0 psi. Because of these concerning preliminary results, computational fluid dynamics (CFD) simulations were run using SolidWorks to determine the effective flow rate and pressure, given the pump's limitations. The piping and nozzles were modeled in SolidWorks, as shown in Figures 4.3 and 4.4, and a fixed pressure and flow rate were provided at the inlet based on the operating pump values.

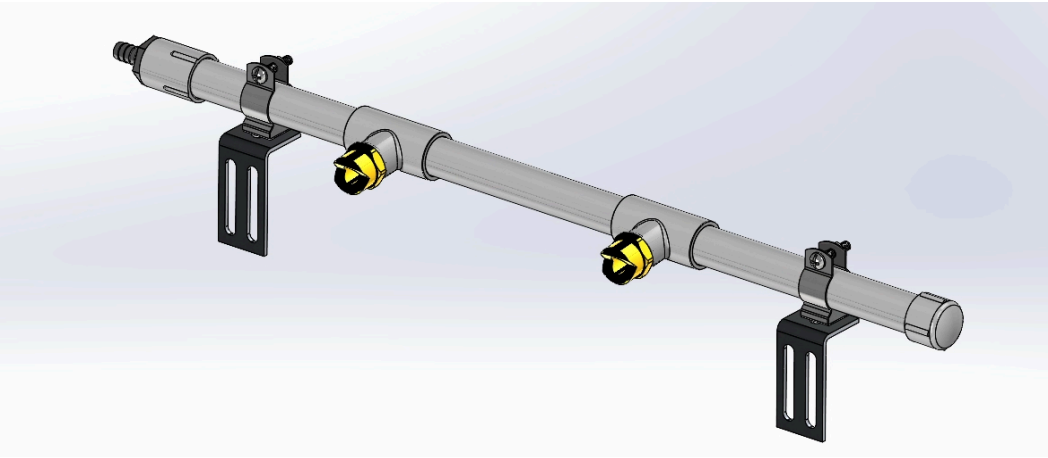

Figure 4.3: SolidWorks CAD Model of PVC piping, nozzles, and mounting brackets. *This model does not show the pump and connecting hose. The brackets are not necessary for this fluid simulation and are purely for visuals.*

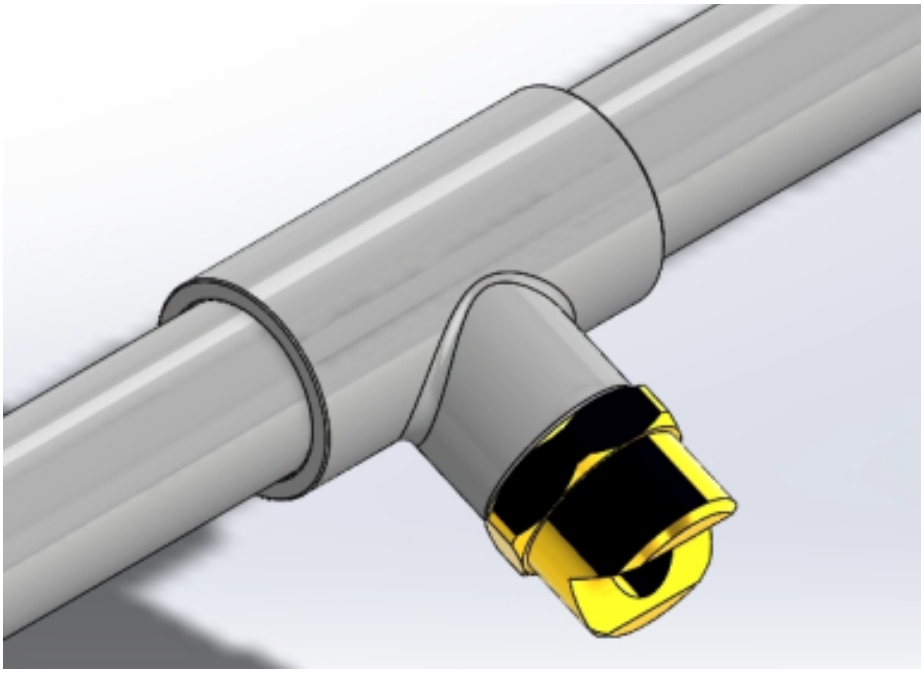

Figure 4.4: Close-up of Nozzles in SolidWorks. *The brass nozzles are connected to the PVC pipe using reducing tee fittings.*

The angle of the nozzles is assumed to be appropriate to evenly distribute over the panels. In other words, the angle of tilt the panels reach throughout the day will not be considered enough of an obstruction to change the calculations. The water will be treated as a steady-state flow, and will not account for the time needed to “prime” the pump. In other words, the flow will be treated as a “fully developed flow”.

Both simulations were tested using the standard “water” fluid in SolidWorks. The first simulation run consisted of an inlet flow rate at the barbed hose fitting of 1.5 gal/min or 5.775 in^3/s. The boundary conditions at the outlets of the nozzles were set to environmental pressure conditions. A mesh level of 4 was used. For the second simulation, the outlet boundary conditions and mesh level were kept the same, but the inlet boundary condition was instead set to a pressure of 65 psi.

4.4.3 Results

For the first simulation, using an inlet volumetric flow rate of 5.775 in^3/s, the volumetric flow rate at each nozzle was 9e-9 in^3/s or approximately 0 gal/min (**Figure 4.5**). The pressure at the nozzle outlets was 16.45 psi. One interesting result was that the nozzle closest to the inlet fitting had a wider spray than the nozzle further away, as shown in **Figure 4.6**. Although both nozzles had slightly different pressure trajectories, their outlet pressures remained the same.

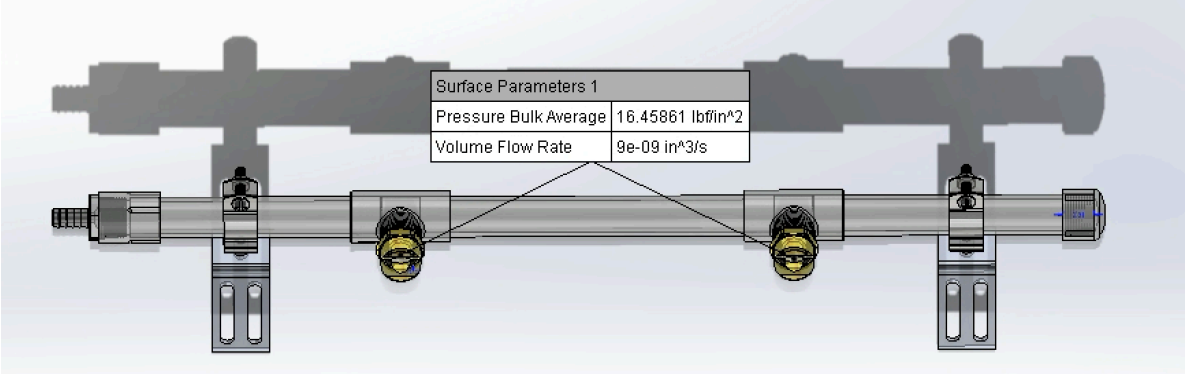

Figure 4.5: Pressure and Volumetric Flow Rate at Nozzle Outlets for Inlet Volumetric Flow Rate of 1.5 gal/min. *The pressure at the nozzles was 16.45, and the flow rate was 9e-9in^3/s.*

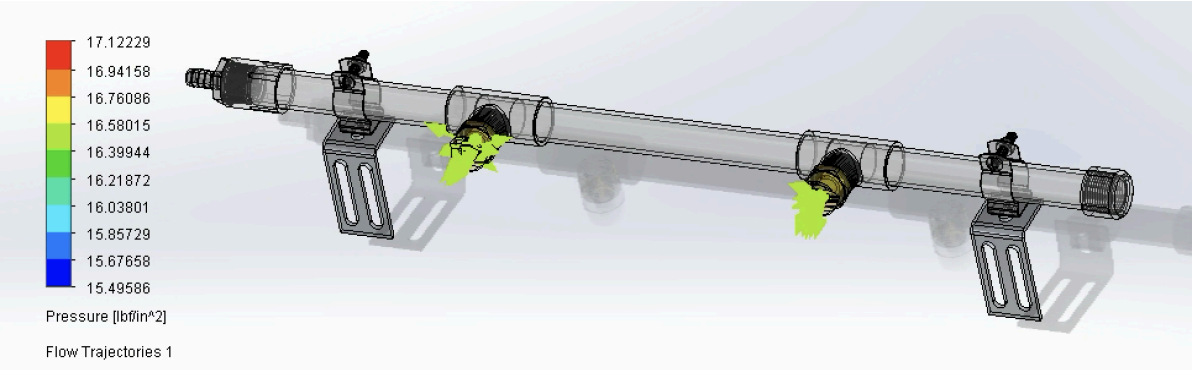

Figure 4.6: Pressure Trajectory at Nozzle Outlets for Inlet Volumetric Flow Rate of 1.5 gal/min. *The left nozzle has a wider spray, and the right nozzle's pressure trajectory is more direct and compact.*

For the second simulation, with an inlet pressure of 65 psi, the volumetric flow rate at each nozzle outlet was -3e09 in^3/s or -7.792e-10 gal/min, and the outlet pressure was 16.45 psi (**Figure 4.7**). Interestingly, the outlet pressure did not change significantly across the two simulations. However, the direction of the pressure trajectories did change, with the furthest nozzle now having a trajectory going against the outlet (**Figure 4.8).** This direction change likely corresponds to the negative flow rate of -3e9 in^3/s.

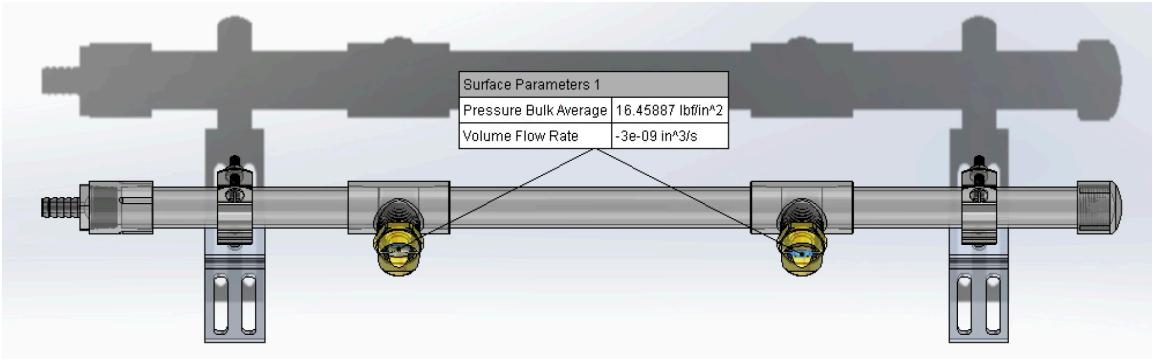

Figure 4.7: Pressure and Volumetric Flow Rate at Nozzle Outlets for Inlet Pressure of 65 psi. *The pressure at the nozzles was 16.45, and the flow rate was -3e-9 in^3/s*

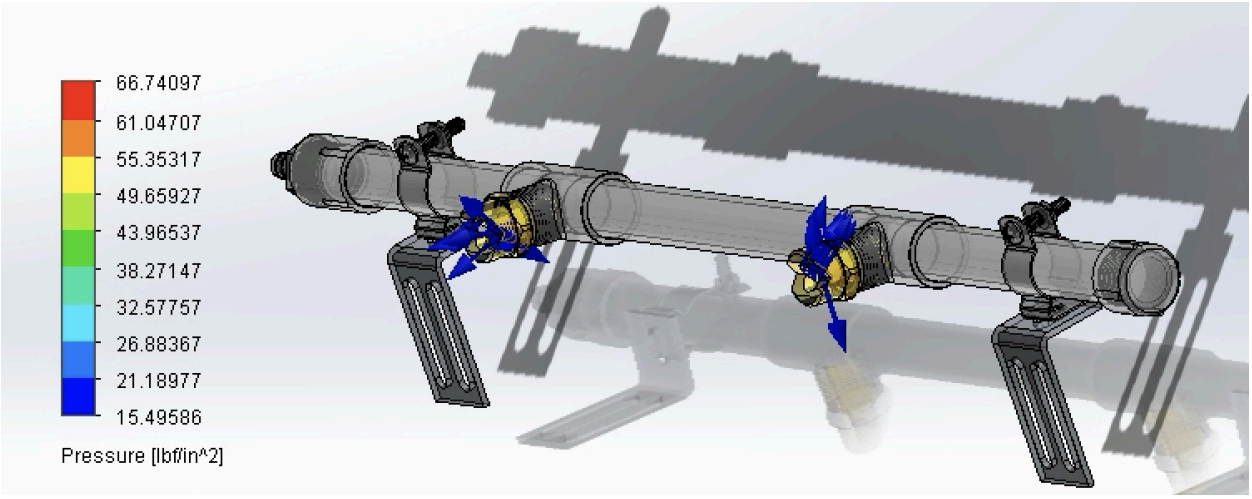

Figure 4.8: Pressure Trajectory at Nozzle Outlets for Inlet Pressure of 65 psi. *The left nozzle has a wider spray, but the right nozzle has arrows pointing inward towards the system.*

4.4.4 Discussion and Design Impact

The first simulation confirmed that an inlet flow rate of 1.5 gal/min would be too low to effectively pass water through the nozzles and clean the panels. The difference in pressure trajectory across the nozzles will affect their spacing, especially when considering the spacing between them and the distance from the end cap, in order to ensure an even spray of water across the panels in the final design. The second simulation also confirmed that the pressure would not work with the current nozzles. The negative flow rate shows that there is likely some sort of vortex action happening. However, further studies could be done to model the whole system, including the hose that connects the pump to the barbed hose fitting.

Given that the nozzles are rated for a higher flow rate at a lower pressure (6 gal/min at 40 psi), the nozzles will either need to be swapped out or the geometry of the piping should be changed, such as using a different pipe schedule. The assumptions also likely affected the results, showing a more optimistic result than what would actually occur, due to the assumed fully-developed flow. These CFD simulations validated the preliminary results calculated, and suggest that the nozzles and pump are indeed poorly matched and will not meet the flow rate and pressure required to clean debris off the panel. In fact, the system performed so poorly that there is also no likelihood of damaging the panels or any coatings.

Next steps will include simulating with different nozzles specifically designed for low flow and high pressure to match that of the pump, as well as simulating different spacings and pipe schedules. Another possible design change would be simulating different numbers of nozzles and examining the performance between 1, 2, and 3 nozzles.

4.4.5 Physical Prototyping and Demonstration

To validate the basic functionality of the subsystem, a physical prototype of the sprinkler and hose was constructed and tested independently of the main solar panel holder. This allowed for a direct assessment of the pump-to-nozzle compatibility. The prototype consisted of the PVC pipe, brass nozzles, and a barbed adapter connected to one end of the rubber hose connected to the 12V diaphragm pump (**Figure 4.9**). The scope of this test was primarily qualitative; no formal flow rate measurements were recorded. The main goal of this prototype was to determine "proof of flow" rather than the approximately 0 gal/min calculated during the CFD simulations.

Figure 4.9 The Physical Self-Cleaning Prototype Mounted to the End of the Panel Holder

The demonstration successfully confirmed that the pump and nozzles are compatible. Upon being powered, the pump successfully delivered water through the nozzles and produced a steady stream of water. However, some key improvements need to be made. A leak at the junction between the rubber hose and the PVC barbed adapter will need to be sealed properly before quantitative testing of the system can begin. The system was also tested using a direct connection to the battery, which will not be the case in the final product. These connections, as well as the control system using the Raspberry PI, should be implemented to determine power consumption and whether or not there will be a loss in power draw, further limiting flow.

Subsequent testing phases will transition to quantitative analysis. This will include measuring the actual volumetric flow rate at the nozzles and conducting "dirt-removal" trials on the solar panels to calculate the exact percentage of debris cleared per cycle. Cycle timing will also need to be determined using these tests in conjunction with the implementation of the Raspberry PI.

Chapter 5: Controls Subsystem

5.1 Subsystem Design Overview

The control subsystem plays a crucial role in the project, as it's responsible for estimating the sun's position by reading and post-processing the sensor's output, and controlling the solar panel's position based on the data. This subsystem comprises a sensing module, a microcontroller for processing data, and a command interface to send commands to the linear actuators. The final solution is based on the Raspberry Pi for high-level computation and user interaction. The low-level operations are controlled using Arduino Nano ESP32, which collects the sensor data and commands linear actuator movements. The subsystem is not limited to microcontrollers; it also includes other electronic components, such as a 12V battery, a charge controller, and a buck converter. They are essential parts to keep the ATLAS electrical system up and running.

The main goal of this subsystem is to detect a shadow on one of the photoresistors and rotate the solar panels towards the location to eliminate the shadow and hence turn the solar panels perpendicular to the sun. This is a closed-loop system that controls the single-axis motion, and below is the block diagram explaining the algorithm in detail.

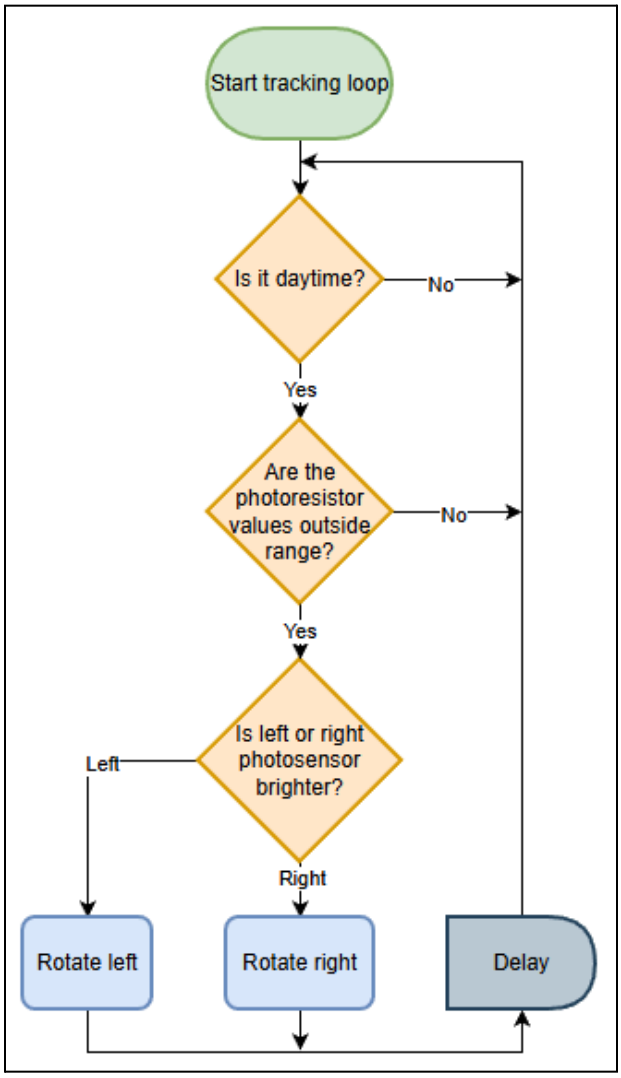

Figure 5.1: Tracking system flowchart

5.2 Tradeoff Analysis and Design Motivation

The sensing module went through several changes related to the design changes made to the ATLAS. First of all, the number of photoresistors was reduced from 4 to 2 since the tracking was simplified from 2 axes to a single axis. This helps not only to make the sensing module cheaper but also more compact and simple to operate.

The previous team was using a Raspberry Pi to control the whole system, but our team decided that using an Arduino Nano ESP32 for low-level analog sensing and linear actuator control was more practical. The Raspberry Pi functionality is now limited to high-level processing and communication with the user.

The final design decision relevant to this subsystem was a conclusion from the electrical testing. The noise was introduced into the LDR signal because the 5V mini solar cell was integrated into the shared rail. To eliminate this issue, the mini solar cell output was moved to a separate analog input of the Arduino microcontroller, and the LDR was isolated on a regulated 3.3 V rail.

5.3 Product Design Review

5.3.1 Sensor Module Design

As discussed earlier, the sensor module contains two photoresistors, which are separated by the divider wall inside a very compact enclosure. If both sensors are well-lit, the system assumes that the solar panel is facing the sun. If one sensor receives less light than the other, ATLAS decides that the shadow is present on the sensor and hence the sun is misaligned, and corrective motion is required. Two figures are presented below. Red-colored entities represent conceptual models of photoresistors. The transparent material is acrylic, and the white material is PLA plastic.

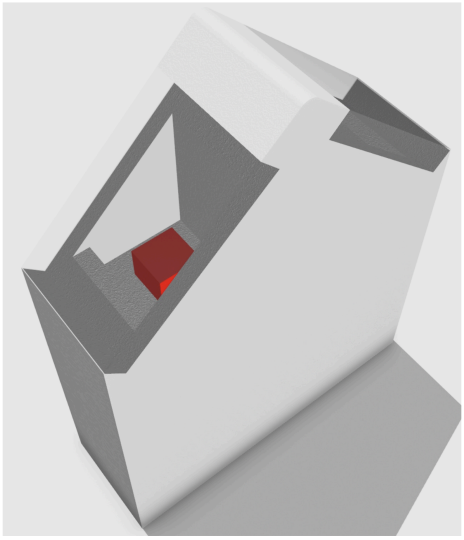

Figure 5.2: Final sensor module used by the controls subsystem

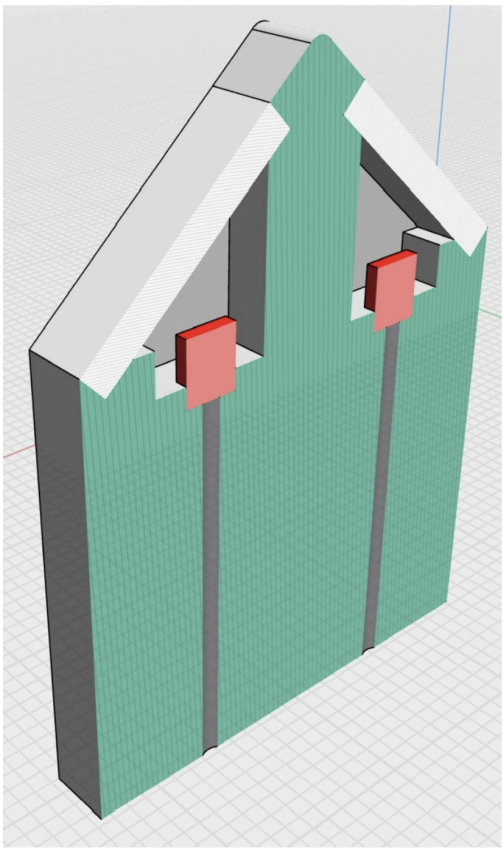

Figure 5.3: Internal sensor geometry showing divider placement and photoresistor layout

5.3.2 Optical Geometry and Simulation

The optical design of the sensor enclosure target is to create directional shading that can be detected. A CAD simulation was used to evaluate the results of the trigonometric calculations. Based on the calculation of capture fraction, a 10-degree misalignment was the minimum misalignment threshold that started to impact the efficiency in a significant way.

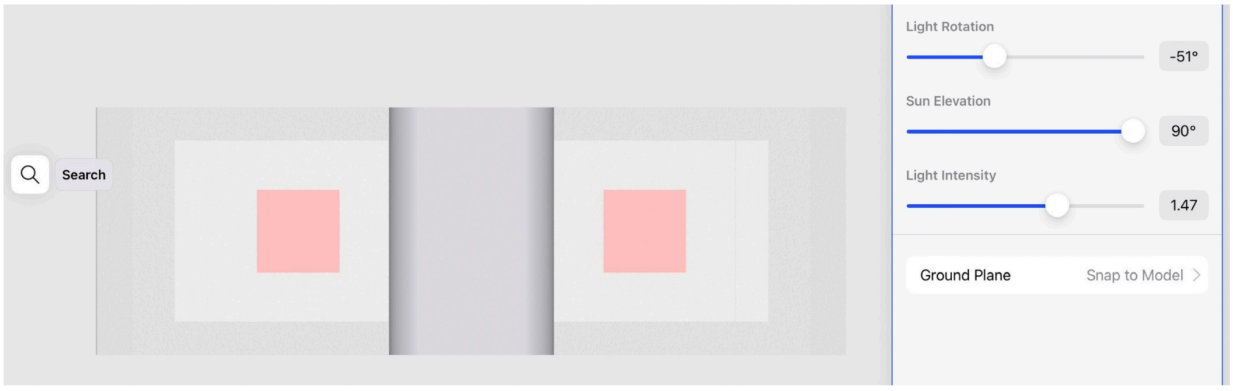

Figure 5.4: CAD simulation at 0° misalignment showing equal illumination

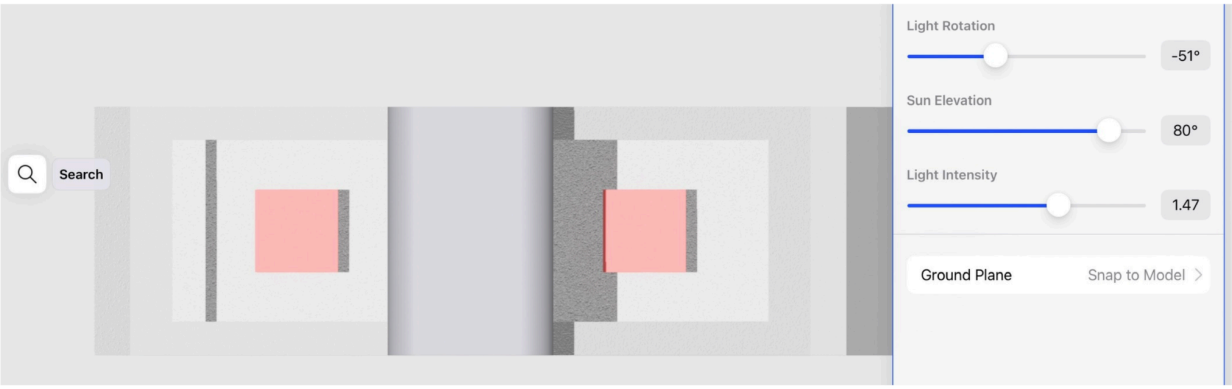

Figure 5.5: CAD simulation at 10° misalignment showing partial shading of one sensor

5.3.3 Processing and Electrical Design

As discussed earlier, the processing hardware is based on Arduino NANO ESP32 and Raspberry Pi. Arduino operates on 3.3 V circuits, and hence the mini solar cell output was reduced from 5 V to 3.33 V using the asymmetrical resistor-divider design, which is within a safe input voltage range for Arduino NANO.

5.3.4 Actuator Control Validation

Another part of the design considered is a linear actuator interface. A technical design review and minimum viable prototype experiment was conducted on the ability of the operator to control the linear actuator, which proves that the motion can be controlled using the current ATLAS electronic hardware package. The experiment showed that the prototype can receive commands from the user and convert it into an analog signal to retract or extend the linear actuator, which also responded as expected.

Figure 5.6: Panel rotating successfully about the intended single axis during the testing.

5.4 Design Investigations and Results

5.4.1 Optical Performance Validation

The first design investigation focused on the optical capabilities of the sensor module geometry. CAD simulation shows that an increase in misalignment angle increases the difference in sensor coverage. At the misalignment angle of 10 degrees, the difference in shadow covering is barely measurable, and the shadow coverage at 20 degrees is total, meaning that sensor module geometry allows for measuring the misalignment from 10 to 20 degrees, which is the exact range it was designed to work in.

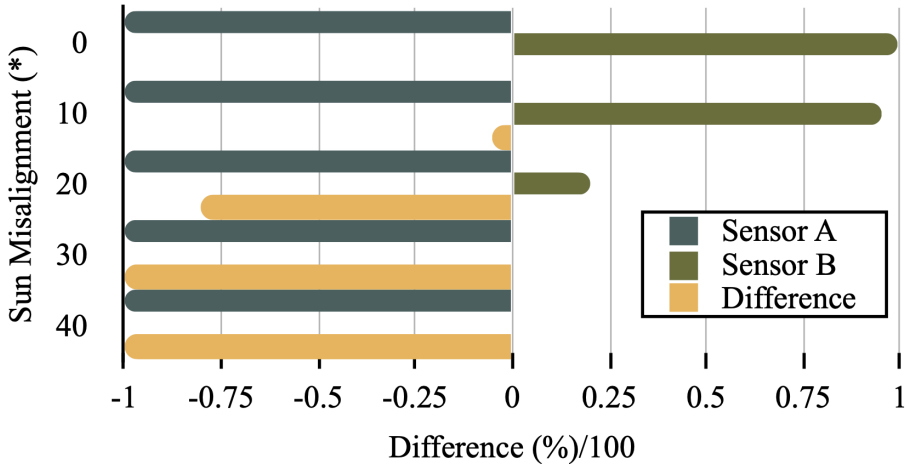

Figure 5.7: Plot of Sun Misalignment Angle (°) vs Exposure Difference (%).

5.4.2 Seasonal / Latitude Robustness

Another important design factor was the seasonal deviation of the sun in terms of latitude. To counter that, side walls were designed with the target to allow the geometry to still work reliably with the latitude misalignment of 20 degrees. The CAD simulation was conducted to evaluate the design, and the simulation confirmed that side walls preserve geometry functionality at the target latitude misalignment.

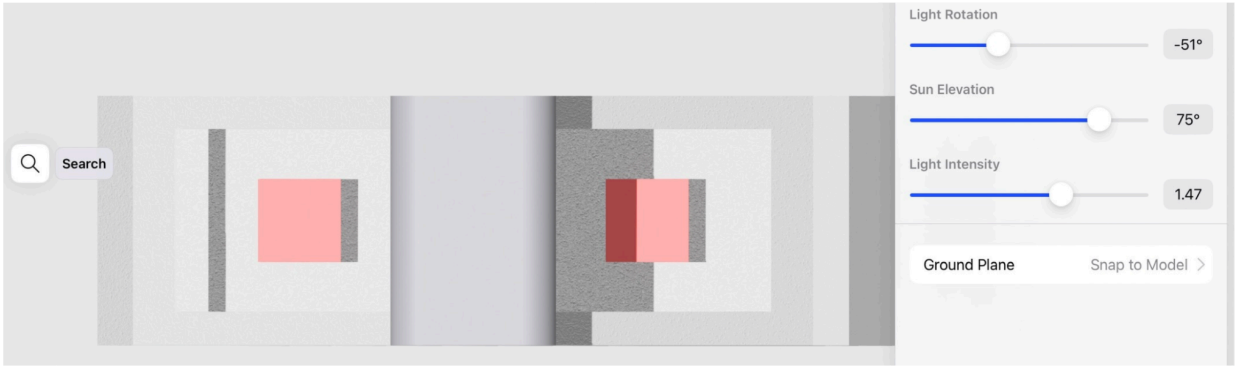

Figure 5.8: Shadow at sun elevation of 75 degrees and latitude angle of 0 degrees

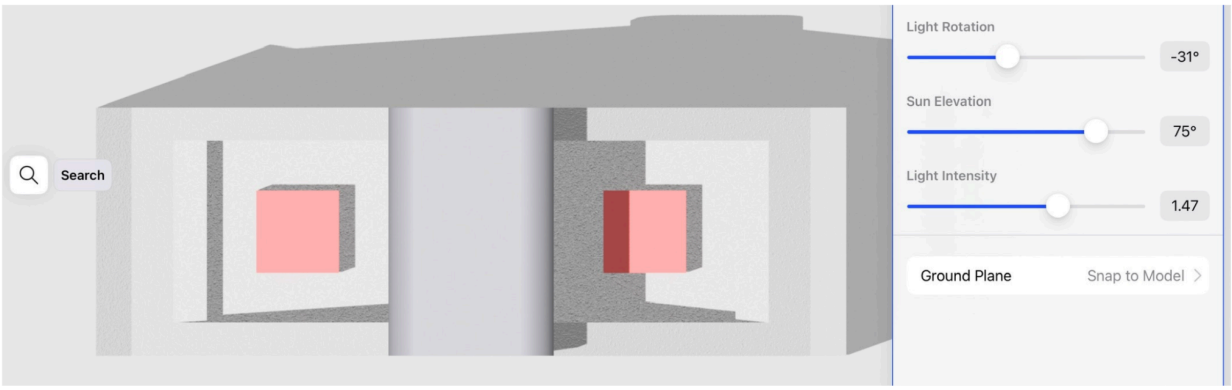

Figure 5.8: Shadow at sun elevation of 75 degrees and latitude angle of 20 degrees

5.4.3 Waterproofing Test

One of the design requirements for the sensor module was waterproofing, since the environmental factors, such as rain, can damage the electronics inside the enclosure, which is 3D printed out of PLA plastic for the body, and the windows are made out of laser-printed acrylic sheet. Enclosure is assembled using a super glue since it's cheap, compatible with both materials, and safe to apply. The waterproofing test was conducted to evaluate whether the enclosure can withstand rain conditions. To indicate the leakage, 4 water-sensitive stickers were placed inside the enclosure, which will turn red if water gets to them or the humidity reaches near saturation. To simulate rain, the enclosure was sprayed 50 times, and all the stickers remained white, meaning that the enclosure is properly sealed from the outside environment.

Figure 5.9: Sensor module interior prior to water exposure.

Figure 5.10: Sensor module interior after 50 spray cycles. No color change observed on water-sensitive labels, confirming absence of leakage.

5.4.4 Electrical Performance and Threshold Logic

Another investigation was conducted on electrical performance. The idle electrical system power draining was evaluated to be 1.49 W based on 0.2 A current and 12.42 V voltage, which is below the 3 W maximum power drainage limit for low solar activity conditions.

The threshold logic for the control system was also established by the team. A baseline of 3495 ADC counts was recorded. The lower threshold is 2500 counts, and hence the difference is 995 counts, which is above 800 counts target in separation, which ensures that the system can reliably distinguish between operating states.

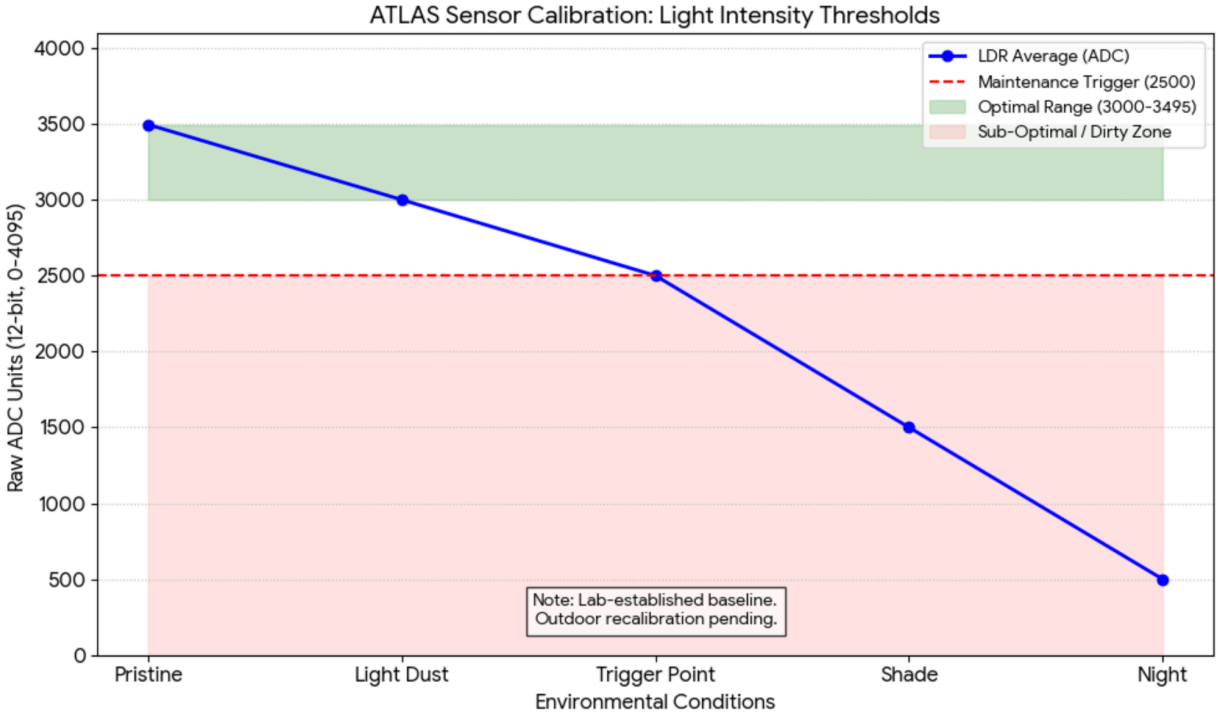

Figure 5.11: Sensor calibration used to define control thresholds and operating logic

5.5 Discussion and Design Impact

The controls subsystem design requirements were evaluated during the tests, and all of them were met successfully without any compromises. The sensor module is waterproof and can successfully read from 10 to 20 degrees of misalignment. The electrical system power drainage in idle stayed beyond the maximum limit, and the system can successfully accept and execute ATLAS movement commands. These results show that the control subsystem is validated at prototype level and ready to be integrated into the ATLAS assembly for further development and testing.

One shortcut was made in order to complete tasks on time. CAD simulation was used to evaluate optical design requirements, but real outdoor testing is required to truly evaluate the design performance.

Chapter 6: Future Work, Expected Budget, and Project Timeline

6.1 Winter Quarter Summary

Winter quarter focused on advancing all three primary subsystems from conceptual design to functional MVP prototypes. The rotation mechanism was fabricated and tested, confirming the linear actuator geometry and actuator range. The self-cleaning manifold was built and validated for flow distribution and solenoid control. The controls system was implemented in Python, with the tracking algorithm and cleaning sequencer both verified independently and integrated. The team also updated the BOM to reflect actual component procurement and refined cost projections for Spring fabrication.

6.2 Bill of Materials and Budget

Table 6.1 presents the current budget status and projected costs for remaining Spring quarter work. Electrical and hardware expenditures to date total approximately $2,303.19, within the School of Engineering procurement limits. Spring quarter costs are primarily driven by final actuator hardware, enclosure components, and integration materials.

Table 6.1: Budget Summary and Spring Quarter Cost Projections

Category	Estimated Cost	Notes
Linear Actuators	$60-$120 each	Based on subsystem selection; 2 per module
Machined/Printed Brackets	$50-$150	Mounting hardware and hinge components
Cleaning Manifold	$40-$100	PVC/PEX distribution components
Solenoid Valve + Fittings	$20-$45	Cleaning subsystem flow control
Electronics Enclosure	$40-$80	Outdoor-rated, IP65 compliant
Contingency	~$100	Standard design buffer
Electrical (to date)	**~$889.52**	**Within School of Engineering limits**
Hardware (to date)	**~$1,413.67**	
TOTAL TO DATE	**~$2,303.19**	
PROJECTED FINAL	**$2,600-$2,800**	

6.3 Project Timeline

6.3.1 Winter Quarter Milestones (Completed)

Table 6.2: Winter Quarter Milestone Schedule

Weeks	Winter Quarter Milestones
Wk 1-2	Finalize actuator geometry, spacing assumptions, and kinematic model
Wk 3-4	Structural FEA on brackets and frame; BOM finalization
Wk 5-6	Frame fabrication and bracket manufacturing
Wk 7-8	Mechanical assembly and actuator installation; initial rotation tests
Wk 9	Cleaning manifold construction and bench validation
Wk 10	Electronics integration, Python control loop implementation, dry-run testing

6.3.2 Spring Quarter Plan

Table 6.3: Spring Quarter Milestone Schedule

Weeks	Spring Quarter Milestones
Wk 1-2	Full electrical integration and system-level debugging
Wk 3	Cleaning subsystem outdoor validation and cleaning angle optimization
Wk 4-5	Outdoor solar tracking performance testing and control algorithm calibration
Wk 6-7	Data collection, energy yield analysis, and system refinement
Wk 8-9	Final report writing, documentation, and poster creation
Wk 10	Senior Design Day presentation and project closeout

6.4 Remaining Work and Open Items

Three primary workstreams remain for Spring quarter:

- Outdoor Performance Validation: Full-system testing under real solar conditions to quantify tracking efficiency gain relative to a fixed reference panel. Target: demonstrate greater than 20% energy yield improvement (FR-01, PR-01).
- Cleaning System Verification: Quantitative outdoor measurement of panel efficiency before and after automated cleaning cycles. Target: confirm 10% or greater efficiency recovery (PR-03).

- Integration and Reliability Testing: Continuous operation testing over multiple days to verify that tracking, cleaning, and communication functions operate reliably within a unified control loop under varying environmental conditions.

6.5 Summary

Winter quarter successfully transitioned ATLAS from conceptual design to prototyped, individually tested subsystems. Spring quarter work is focused on full-system outdoor validation, quantitative performance verification against the requirements in Table 2.1, and preparation of final deliverables. The project remains within budget and on schedule for Senior Design Day in Spring 2026.

References

[1] A. Geetha et al., "Dust accumulation and its impact on solar panel efficiency," Renewable Energy Reviews, 2024.

[2] J. Harazin and A. Wrobel, "Analysis and study of the potential increase in energy output generated by prototype solar tracking, roof-mounted solar panels," F1000Research, vol. 9, p. 1381, Jul. 2022. doi:10.12688

[3] D. Li et al., "Compressed air cleaning for solar panels: efficiency analysis," Solar Energy, 2021.

[4] M. A. Ismail et al., "Arduino-based dual-axis solar tracking system," International Journal of Engineering, 2020.

[5] Z. Almusaied et al., "Effect of panel orientation and cleanliness on photovoltaic output," Energy Procedia, 2018.

[6] W. J. C. Melis et al., "Water cooling for solar panel thermal management," Applied Energy, 2014.

[7] N. Najmi and A. Rachid, "A Review on Solar Panel Cleaning Systems and Techniques," Energies, vol. 16, no. 24, 2023, article 7960. doi:10.3390/en16247960

[8] TattvaTech, "Automatic Solar Panel Cleaning System," 2025, https://www.tattvatech.in/product_range/automatic-solar-panel-cleaning-system/

[9] “Best MULTIFIT MR-G2 solar panel cleaning machine automatic cleaning robot for solar cell energy system cleaning robot manufacturer and factory: Multifit,” 2025, https://www.vmaxpowerpv.com/multifit-solar-panel-cleaning-machine-automatic-cleaning-robot-for-solar-cell-energy-system-cleaning-robot-product/

[10] Call Sun Solar, "100W P-Type Solar Panel Specifications," Call Sun Solar, Tech. Spec. Sheet, 2024. [Online].

[11] R. Berendsohn, "Pressure Washer GPM vs. PSI: Which Is More Important?" Popular Mechanics, Jan. 14, 2025. [Online].